

Article

Open Access

# Molecular phylogeny and taxonomy of four *Remanella* species (Protozoa, Ciliophora): A flagship genus of karyorelictean ciliates, with descriptions of two new species

Ming-Zhen Ma<sup>1,#</sup>, Yu-Jie Liu<sup>1,#</sup>, Yuan Xu<sup>2</sup>, Bo-Rong Lu<sup>1</sup>, Yu-Qing Li<sup>1</sup>, Saleh A. AL-Farraj<sup>3</sup>, Giulio Petroni<sup>4</sup>, Wei-Bo Song<sup>1,5</sup>, Ying Yan<sup>1,\*</sup>

<sup>1</sup> Institute of Evolution & Marine Biodiversity, Ocean University of China, Qingdao, Shandong 266003, China

<sup>2</sup> State Key Laboratory of Estuarine and Coastal Research, East China Normal University, Shanghai 200241, China

<sup>3</sup> Zoology Department, College of Science, King Saud University, Riyadh 11451, Saudi Arabia

<sup>4</sup> Department of Biological, University of Pisa, Pisa 56100, Italy

<sup>5</sup> Laboratory for Marine Biology and Biotechnology, Qingdao National Laboratory for Marine Science and Technology, Qingdao, Shandong 266237, China

## ABSTRACT

During faunal studies of psammophilic ciliates along the coast of Qingdao, China, several marine karyorelictean species were isolated. Among them, four species within the genus *Remanella* were investigated, including two species new to science: i.e., *R. rugosa*, *Remanella elongata* **sp. nov.**, *Remanella aposinica* **sp. nov.**, and *R. unicorpusculata*. *Remanella rugosa* has been reported several times, but this study is the first to provide detailed morphological characters and phylogenetics. *Remanella elongata* **sp. nov.** can be distinguished from its congeners by the presence of complex cortical granules, fewer macronuclei, and longer body size. *Remanella aposinica* **sp. nov.** differs from its congeners by having 14–17 right lateral ciliary rows and 24–37 dikinetids of intrabuccal kinety. Poorly known *Remanella rugosa*

var. *unicorpusculata* (Kahl, 1933) Foissner, 1996 should be elevated from subspecies to species level, *Remanella unicorpusculata* (Foissner, 1996) **stat. nov.**, based on detailed redescriptions with statistical data, living morphology, infraciliature, and species definitions. Small subunit (SSU) rDNA was sequenced for the four species, and phylogenetic analysis revealed that all known taxa in *Remanella* formed the outline branch to the genus *Loxodes* with moderate to high bootstrap support among *Remanella* lineages.

**Keywords:** Marine ciliates; Morphology; Infraciliature; Phylogeny

Received: 07 April 2022; Accepted: 19 August 2022; Online: 22 August 2022

Foundation items: This work was supported by the National Natural Science Foundation of China (32030015, 31961123002, 32111530116), King Saud University, Saudi Arabia (RSP2022R7), Fundamental Research Funds for the Central Universities to Y.Y. (202141007), European Community H2020-MSCA-RISE 2019 (872767), and Young Taishan Scholar Program of Shandong Province

\*Authors contributed equally to this work

\*Corresponding author, E-mail: [yanying@ouc.edu.cn](mailto:yanying@ouc.edu.cn)

This is an open-access article distributed under the terms of the Creative Commons Attribution Non-Commercial License (<http://creativecommons.org/licenses/by-nc/4.0/>), which permits unrestricted non-commercial use, distribution, and reproduction in any medium, provided the original work is properly cited.

Copyright ©2022 Editorial Office of Zoological Research, Kunming Institute of Zoology, Chinese Academy of Sciences

## INTRODUCTION

The enigmatic ciliate class Karyorelictea Corliss, 1974 is widely considered to represent the ancestral ciliate stage (Hu et al., 2019; Lynn, 2008; Song et al., 2009; Wang et al., 2019a; Xu et al., 2013a, 2013b; Yan et al., 2013, 2015, 2016, 2017, 2019) due to various unique features, i.e., numerous non-dividing macronuclei (arising from extra divisions of micronuclei) and somatic ciliation with dikinetids (possessing postciliodesmata). Most karyorelictean ciliates live in marine habitats, typically intertidal sandy beaches, and are a key component of benthic energy transfer (Fenchel & Finlay, 1986; Foissner, 1998; Lynn, 2008; Wang et al., 2019b, 2020). Among marine karyorelicteans, *Remanella* can be well recognized due to its distinct characteristics such as beak-like anterior rostrum and Müller vesicles. To date, 14 nominal species have been assigned to *Remanella* (Xu et al., 2013a), eight of which have not been studied by modern morphological techniques (i.e., silver staining, electron microscopy) or molecular methods, resulting in poor information on ciliary patterns, ultrastructures, morphometrics, and molecular data (Foissner, 1996; Xu et al., 2012, 2013a). Therefore, further research on *Remanella* is required. As more molecular data become available for karyorelicteans and more integrative morphological studies have been performed (e.g., using living observations, silver staining, and scanning electron microscopy), the inter- and intra-generic relationships within Karyorelictea can be better established (Andreoli et al., 2009; Foissner, 1996; Gao et al., 2010; Mazei et al., 2009; Xu et al., 2012).

In the present study, we report on four *Remanella* species isolated from the intertidal zone of a sandy beach on the coast of Qingdao, China. *Remanella elongata* sp. nov. and *Remanella aposinica* sp. nov. are identified and described as new species. Furthermore, *Remanella rugosa* (Kahl, 1933) Foissner, 1996 is presented in detail and *Remanella unicorpusculata* (Kahl, 1933) stat. nov. is redescribed for the first time, providing details on infraciliature for both species. The molecular phylogeny of the four species was analyzed based on newly sequenced small subunit (SSU) rDNA.

## MATERIALS AND METHODS

### Sample collection, observation, and identification

During ebb tide, ciliates were sampled and isolated from sandy sediment in the intertidal zone of a beach along the coast of Qingdao, China (Figures 1). A 2 cm–3 cm trough was dug, and the top 5 cm of sand and seawater was collected after the trough filled with seawater. Finally, about 10 kg of this mixture was loaded into a bucket. To enrich ciliates in the lab, we used nylon gauze (80 µm–90 µm pore) to filter the collected samples. Firstly, nylon gauze was tied to one end of a polyvinyl plastic tub (50 mm diameter, 100 mm long). About 30 mm of sand was placed in the lower layer of the tube and 30 mm of ice was placed on the upper layer. Seawater and melted freshwater drove the ciliates out of the sand. The filtered samples were collected in Petri dishes (60 mm diameter) (Ma et al., 2021a).

Cells were isolated and observed *in vivo* using bright field

and differential interference microscopy (100× to 1 000× magnifications) with an Olympus BX 53 light microscope (Japan). The infraciliature was revealed using the protargol staining method (Wilbert, 1975). Counts and measurements of impregnated specimens were performed at a magnification of 1 000×. Terminology and systematics primarily followed Foissner (1996) and Lynn (2008), respectively.

### DNA extraction, gene amplification, and sequencing

For each species, a single cell was washed with filtered and autoclaved marine water to exclude contamination. Genomic DNA was extracted using a DNeasy Blood & Tissue Kit (Qiagen, Germany) according to the manufacturer's protocol (Ma et al., 2021a, 2021b). Primers 82F (5'-GAAAC TGCGAATGGCTC-3') (Jerome et al., 1996) and 18S-R (5'-TGATCCTTCTGCAGGTTTCACCTAC-3') (Medlin et al., 1988) were used to amplify SSU rDNA by polymerase chain reaction (PCR). To reduce experimental error caused by PCR, Q5® Hot Start High-Fidelity DNA Polymerase (New England Biolabs, USA) was used to amplify the SSU rDNA. The touchdown PCR procedure was performed as follows: one cycle of initial denaturation at 98 °C for 30 s, followed by 18 cycles of amplification (98 °C, 10 s; 69–52 °C, touchdown, 30 s; 72 °C, 1 min) and another 18 cycles (98 °C, 10 s; 51 °C, 30 s; 72 °C, 1 min), with a final extension of 72 °C for 5 min. The PCR products were purified using an EasyPure Quick Gel Extraction Kit (Transgen Biotech, China), and then cloned using a pClone007 Blunt Simple Vector Kit (Tsingke Biological Technology, China). One clone was randomly selected and cultured in Luria-Bertani (LB) Broth medium for 12 h, then sequenced in two directions by the Tsingke Biological Technology Company (China). The procedure was performed according to Xu et al. (2013a).

### Phylogenetic analyses

In addition to the newly characterized SSU rDNA sequences, 72 sequences were obtained from the NCBI GenBank database. Five heterotrichs were selected as outgroup species. Sequence alignment was carried out using the GUIDANCE algorithm (Penn et al., 2010) with default parameters on the GUIDANCE web server (Penn et al., 2010). The resulting alignment was manually edited using BioEdit v7.0.5.2 (Hall, 1999). The final alignment, including 1 694 sites and 76 taxa, was used to construct phylogenetic trees.

Bayesian inference (BI) analysis was performed with MrBayes v3.1.2 (Ronquist et al., 2012) using the GTR+I+G model as selected by Akaike information criterion (AIC) in MrModeltest v.2.0 (Nylander, 2004). The BI analysis was conducted with 1 000 000 generations and sampling every 100 generations. The first 25% of sampled trees were discarded as burn-in. Maximum-likelihood (ML) analysis was carried out with 1 000 replicates using the CIPRES Portal v2.0 (<http://www.phylo.org>) and RAXML-HPC2 on XSEDE with the GTRGAMMA model (Stamatakis et al., 2008). MEGA v.5.0 (Tamura et al., 2011) was used to visualize phylogenetic tree topology.

### Topology testing

The statistical possibility of alternative phylogenetic hypotheses was evaluated using approximately unbiased (AU)



**Figure 1** Sample sites

A: Green dot shows location of Qingdao. B: Orange dots indicate locations of sampling sites. C: Intertidal zone of sandy beach near First Bathing Beach, Qingdao. D: Intertidal zone of Silver Beach, Qingdao.

tests (Shimodaira, 2002) to assess phylogenetic relationships among different taxa within Karyorelictea. Two constrained ML trees were generated using RAXML v8.2.10 (Stamatakis, 2014) with enforced constraints and then compared with unconstrained ML topologies implemented in CONSEL (Shimodaira & Hasegawa, 2001).

## RESULTS

**Class Karyorelictea Corliss, 1974**

**Family Loxodidae Bütschli, 1889**

**Genus *Remanella* Foissner, 1996**

***Remanella rugosa* (Kahl, 1933) Foissner, 1996 (Figures 2, 3; Table 1)**

This species was first reported by Kahl (1933) based on observations of its living morphology. Several researchers later provided sketches of living species (Carey & Maeda, 1985; Dragesco, 1960; Kattar, 1970). Raikov (1993) described its extrusomes and Foissner (1996) depicted its infraciliature but without detailed description. Therefore, a redescription with observation on both living and stained specimens is needed. Here, we provide an improved diagnosis based on

previous and present observations and a detailed redescription based on the Chinese population.

**Improved diagnosis:** Cell size *in vivo* 90–400  $\mu\text{m}$ ×20–50  $\mu\text{m}$ ; ratio of buccal field/body length about 1/5–1/3; 11–15 right lateral ciliary rows; right buccal, left outer buccal, and intrabuccal kinety composed of 40–60, 14–25, and 23–40 dikinetids, respectively; 2–3 macronuclei; single micronucleus; cortical granules brown; 3–10 Müller vesicles; marine habitat.

**Voucher material:** A voucher slide of protargol-impregnated specimens was deposited in the Laboratory of Protozoology, Ocean University of China (OUC), Qingdao, China (Registration No. MMZ2020060202).

**Description:** Live cells slender and rather flexible, 90–200  $\mu\text{m}$ ×20–50  $\mu\text{m}$ ; most about 110  $\mu\text{m}$ ×35  $\mu\text{m}$  in size, with buccal field occupying ca. 1/5 of body length (Figure 2A–C; Figure 3A, B). Cilia about 6  $\mu\text{m}$  long. Cells mostly dark brown at low magnification due to brown cortical granules. Cortical granules ca. 0.5  $\mu\text{m}$  in diameter and densely packed in buccal area, around pharyngeal tube, and on both cell sides (Figure 2F, G; Figure 3C–E). On right side of cell, cortical granules arranged in lines along ciliary rows (Figure 2G; Figure 3C, E). On left side of cell, cortical granules scattered (Figure 2F;

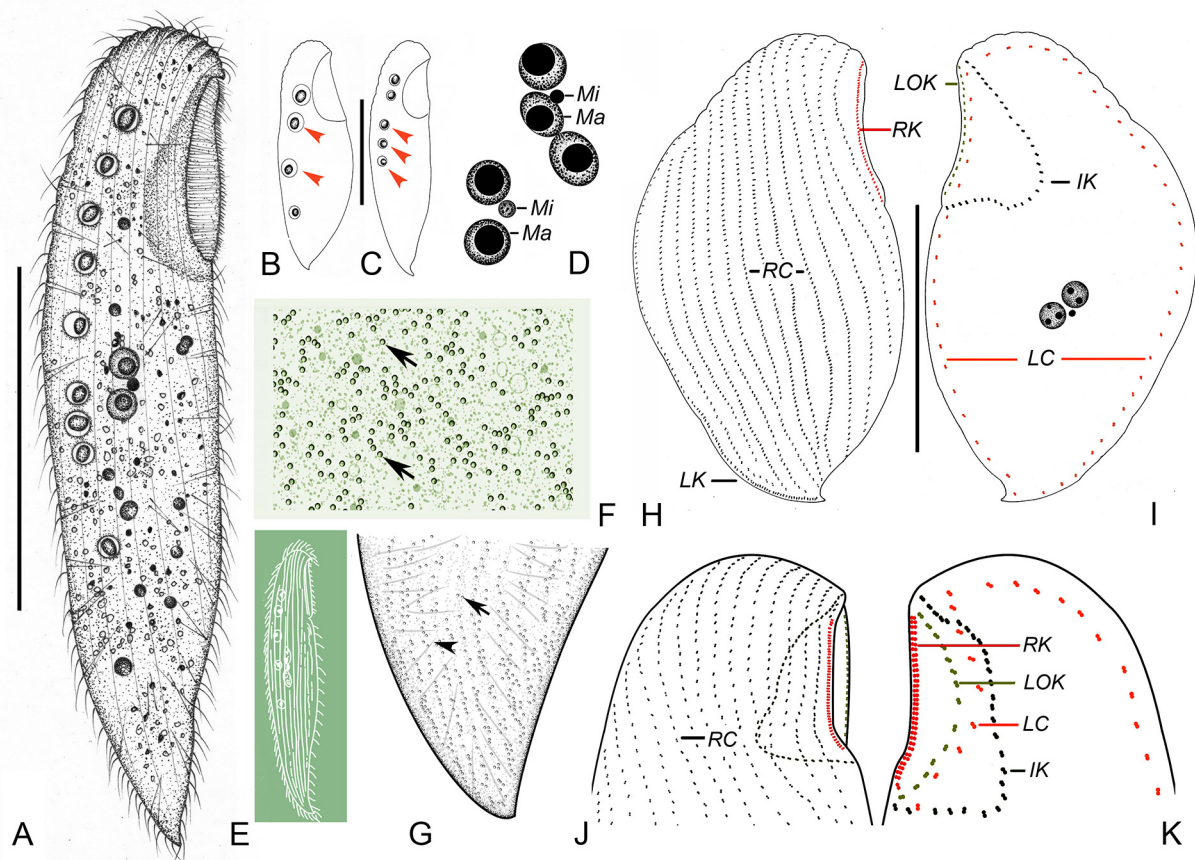


**Figure 2** *Remanella rugosa* (Kahl, 1933) Foissner, 1996 from life (A–G) and after protargol staining (H–K)

A: Representative individual. B, C: Different body shapes. Arrows point to Müller vesicles. D: Variation in composition of nuclear groups. E: *Remanella rugosa* (after Kahl, 1933). F, G: Distribution of cortical granules (arrows) on left (F) and right (G) side. Arrowhead in G showing spicule. H, I: Infraciliature of right (H) and left (I) side of holotype specimen, noting ciliary rows. J, K: Right (J) and left (K) side view of buccal infraciliature. IK, intrabuccal kinety; LOK, left outer buccal kinety; LC, left lateral ciliary row; LK, dorsolateral kinety; Ma, macronuclei; Mi, micronucleus; RC, right lateral ciliary rows; RK, right buccal kinety. Scale bars: 80  $\mu\text{m}$  (A–C); 60  $\mu\text{m}$  (H, I).

Figure 3D). Five to ten Müller vesicles located near dorsal margin of cell, each 7  $\mu\text{m}$  in diameter with a globular or ellipsoidal mineral granule ca. 2  $\mu\text{m} \times 5 \mu\text{m}$  across (Figure 2A–C; Figure 3A, B). Cytoplasmic spicules about 10  $\mu\text{m}$  long, scattered throughout cell (Figure 2A, G; Figure 3A, B, F, H). Many refractive globular granules scattered throughout cell (Figure 3G, H). Two to three macronuclei with single closely associated micronucleus (Figure 2D; Figure 3F, J, K). Locomotion by gliding between sand grains or along bottom of Petri dish.

Entire infraciliature consisting of dikinetids. Right surface densely ciliated with 12–14 right lateral ciliary rows (Figure 2H; Figure 3I, L). Dorsolateral kinety extending to posterior end of cell (Figure 2H; Figure 3I). Left lateral ciliary row extending around entire cell margin (Figure 2I). Right buccal kinety longitudinal along right margin of buccal overture, composed of 40–60 tightly spaced dikinetids (Figure 2J, K; Figure 3M). Left outer buccal kinety longitudinal along left margin of buccal overture, composed of 17–25 closely spaced dikinetids (Figure 2J, K). Intrabuccal kinety consisting of 23–40 dikinetids (Figure 2J, K).

***Remanella elongata* sp. nov. (Figures 4, 5; Table 1)**

**Diagnosis:** Cell size *in vivo* 250–500  $\mu\text{m} \times 50$ –70  $\mu\text{m}$ ; buccal field occupying ca. 1/4–1/3 of body length; 18–22 right lateral ciliary rows; right buccal, left outer buccal, and intrabuccal kinety composed of 125–180, 50–100, and 105–150 dikinetids, respectively; 1–3 macronuclei, single micronucleus; cortical granules tiny, brown, in lines distributed in both sides of glabrous stripe and along ciliary rows, but sparsely in middle of glabrous stripe; 7–13 Müller vesicles. Marine habitat. **Type locality, ecological features, and sample date:** Intertidal zone of Silver Beach at Qingdao (N35°55'09", E120°11'55"), China (Figure 1). Water temperature was 24 °C and salinity was ca. 30‰. Sample was collected on 13 June 2020.

**Type specimens:** A protargol-impregnated slide containing the holotype specimen marked with an ink circle was deposited in the Laboratory of Protozoology, OUC, China (No. MMZ2020061304).

**Etymology:** The species group name “*elongata*” refers to the slender body shape of the species.

**Description:** Live cells 250–500  $\mu\text{m} \times 50$ –70  $\mu\text{m}$ ; most about 400  $\mu\text{m} \times 60 \mu\text{m}$  in size, with buccal field occupying ca. 1/4–1/3

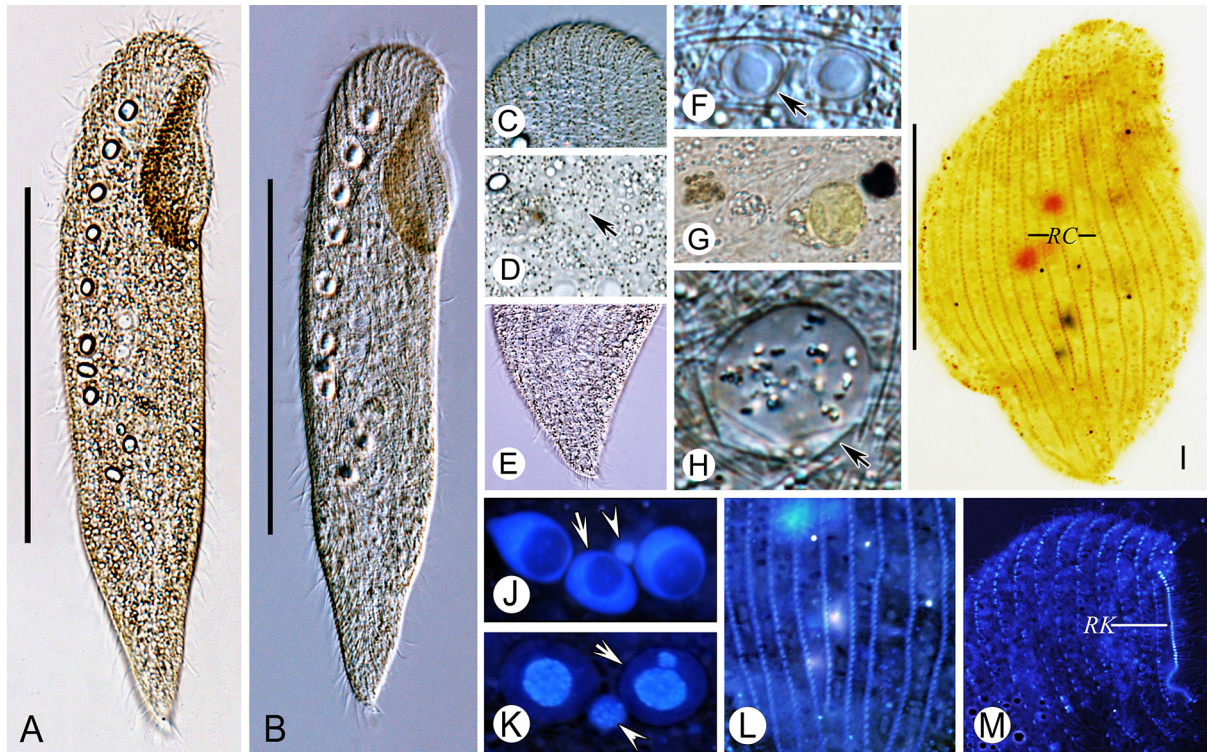


**Figure 3** Photomicrographs of *Remanella rugosa* (Kahl, 1933) Foissner, 1996 from life (A–H) and after protargol staining (I–O)

A, B: Typical individuals. C: Distribution of cortical granules of anterior region on right side. D: Distribution of cortical granules of middle region on left side. E: Distribution of cortical granules of end region on right side. F: Nuclear group, arrow marks macronucleus. G, H: Inclusions and granules. I: Infraciliature of right side of holotype specimen. J, K: Nuclear groups by invertible function in Photoshop. Arrows point to macronuclei; Arrowheads point to micronuclei. L: Right lateral ciliary rows based on invertible function in Photoshop. M: Right side view of anterior body region based on invertible function in Photoshop. RC, right lateral ciliary rows; RK, right buccal kinety. Scale bars: 80  $\mu\text{m}$  (A, B); 60  $\mu\text{m}$  (I).

of body length (Figure 4A–D; Figure 5A–E). Cilia about 10  $\mu\text{m}$  long. Cells brown at low magnification ( $\times 50$ ) due to many rows of highly refractile cortical granules. Cells appearing dark at mid-body, with transparent anterior and tail at low magnification due to presence or absence of multiple refractile particles. Cortical granules tiny (ca. 0.5  $\mu\text{m}$  in diameter), brown, in lines on both sides of glabrous stripe. Longitudinal bright “line” appearing due to sparsely scattered cortical granules in middle of glabrous stripe. Cortical granules densely covering margin in left lateral region of cell (Figure 4E, G; Figure 5G, H). Approximately 7–13 Müller vesicles for gravity reception, 10  $\mu\text{m}$  in diameter, with globular or ellipsoidal mineral content ca. 5  $\mu\text{m}$  in diameter, located near dorsal margin, mostly gathering at anterior; several small developing Müller vesicles dispersed in cell (Figure 4A–D, I; Figure 5A–F). Spicules forming unique cytoskeleton, most about 15  $\mu\text{m}$  long, scattered throughout cell (Figure 4A, I; Figure 5F, L). Food vacuole observed with diatom inside (Figure 5I), suggesting consumption of diatoms. Glides through sand grains and on bottom of Petri dish, sometimes undulating.

Infraciliature consisting of dikinetids. Right surface densely ciliated, gradually shortening anteriorly at posterodorsal margin of cell, especially posteriorly at ventral margin, with 18–22 right lateral ciliary rows (Figure 4J; Figure 5P). Dorsolateral kinety extending to end of tail (Figure 4J). Left

side barren. Left lateral ciliary row curving around cell (Figure 4K; Figure 5K). Right buccal kinety longitudinal along right margin of buccal overture, composed of 125–180 tightly spaced dikinetids (Figure 4H; Figure 5J, O). Left outer buccal kinety longitudinal along left margin of buccal overture, composed of 50–100 closely spaced dikinetids (Figure 4H; Figure 5J, N). Intra-buccal kinety consisting of 105–150 dikinetids (Figure 4H; Figure 5J, O). One to three macronuclei with single micronucleus in-between (Figure 4F; Figure 5L, M).

#### *Remanella aposinica* sp. nov. (Figures 6, 7; Table 1)

**Diagnosis:** Cell size *in vivo* about 160–285  $\mu\text{m} \times 35$ –55  $\mu\text{m}$ ; buccal field occupying ca. 1/6–1/5 of body length; 14–17 right lateral ciliary rows; right buccal, left outer buccal, and intra-buccal kinety composed of 75–105, 15–25, and 24–37 dikinetids, respectively; 2–3 macronuclei; single micronucleus; brown cortical granules; single Müller vesicle. Marine habitat.

**Type locality, ecological features, and sample date:** Intertidal zone of First Bathing Beach at Qingdao (N36°03'24", E120°20'32"), China (Figure 1). Water temperature was 20 °C and salinity was ca. 30‰. Sample was collected on 6 March 2019.

**Type specimens:** A protargol-impregnated slide containing the holotype specimen marked with an ink circle was deposited in the Laboratory of Protozoology, OUC, China (No. MMZ2019030601).

**Etymology:** The epithet is composed of the Greek prefix ἀπό

**Table 1** Morphometric data for *Remanella rugosa* (*R. rug*), *Remanella elongata* sp. nov. (*R. elo*), *Remanella aposinica* sp. nov. (*R. apo*), and *Remanella unicorpusculata* (Foissner, 1996) stat. nov. (*R. uni*)

Character	Species	Min	Max	Mean	SD	CV	<i>n</i>
Body length (µm)	<i>R. rug</i>	70	175	110.4	29.1	26.4	25
	<i>R. elo</i>	210	370	285.8	41.5	14.5	25
	<i>R. apo</i>	160	285	231.0	36.7	15.9	20
	<i>R. uni</i>	90	135	114.2	13.7	12.0	25
Body width (µm)	<i>R. rug</i>	25	50	35.0	7.1	20.2	25
	<i>R. elo</i>	35	80	50.2	12.7	25.3	25
	<i>R. apo</i>	35	55	44.8	6.4	14.3	20
	<i>R. uni</i>	10	25	16.2	4.2	25.6	25
Buccal area length (µm)	<i>R. rug</i>	16	35	25.2	5.6	22.3	25
	<i>R. elo</i>	65	110	82.5	12.5	15.2	20
	<i>R. apo</i>	30	60	41.5	7.3	17.7	20
	<i>R. uni</i>	12	30	17.8	4.3	24.2	21
Right lateral ciliary rows (No.)	<i>R. rug</i>	12	14	12.7	0.8	5.9	13
	<i>R. elo</i>	18	22	19.5	1.1	5.8	11
	<i>R. apo</i>	14	17	15.4	0.9	5.9	19
	<i>R. uni</i>	7	10	7.9	0.8	10.6	22
Dikinetids in right buccal kinety (No.)	<i>R. rug</i>	40	60	48.8	6.2	12.7	10
	<i>R. elo</i>	125	180	143.5	16.5	11.5	10
	<i>R. apo</i>	75	105	85.4	8.1	9.5	18
	<i>R. uni</i>	20	33	25.4	4.1	16.0	17
Dikinetids in left outer buccal kinety (No.)	<i>R. rug</i>	17	25	20.5	2.5	12.4	10
	<i>R. elo</i>	50	100	70.2	16.2	23.1	10
	<i>R. apo</i>	15	25	21.3	4.6	21.5	18
	<i>R. uni</i>	3	5	4.1	0.8	20.1	8
Dikinetids in intrabuccal kinety (No.)	<i>R. rug</i>	23	40	29.0	5.4	18.8	11
	<i>R. elo</i>	105	150	131.0	12.9	9.8	10
	<i>R. apo</i>	24	37	31.2	4.6	14.7	10
	<i>R. uni</i>	9	20	12.1	3.2	26.9	10
Macronuclei (No.)	<i>R. rug</i>	2	3	2.3	0.5	20.7	13
	<i>R. elo</i>	2	3	2.3	0.5	20.6	11
	<i>R. apo</i>	2	3	2.2	0.4	17	20
	<i>R. uni</i>	2	3	2.3	0.5	20.7	21

All data are based on protargol-impregnated specimens. Measurements are in µm. CV: Coefficient of variation (%); Max: Maximum; Mean: Average; Min: Minimum; *n*: No. of specimens investigated; SD: Standard deviation of the mean.

(apo, derived from) and species group name *sinica*, reflecting the superficial similarity of this species to *R. sinica* Xu et al., 2012.

**Description:** Live cells 160–285 µm×35–55 µm, most about 200 µm×35 µm in size, with buccal field occupying ca. 1/6–1/5 of body length (Figure 6A, B; Figure 7A, B), narrow due to flattening organism. Tail short and inconspicuous (Figure 7E). Cilia about 10 µm long. Cells rather dark, almost brown due to brown cortical granules ca. 0.5 µm in diameter and densely packed in buccal area, around pharyngeal tube, and on both cell sides except mid-region of left side (Figure 6G–I; Figure 7D, G). Cortical granules conspicuously absent from longitudinally oriented “groove” formed by many transverse folds on left side, appearing as bright “line” when observed *in vivo* (Figure 6I; Figure 7G). On right side of cell, granules arranged in lines along ciliary rows (Figure 6H). Single Müller vesicle about 8 µm in diameter, with globular mineral granule inside, located near dorsal margin of cell, level with posterior

end of buccal area (Figure 6A–C; Figure 7A–C). Cytoplasmic spicules about 10 µm long, scattered throughout cell (Figure 7K, N). Alga observed in body (Figure 7F). Cell surface of left side rather rough due to many transverse folds (Figure 6I; Figure 7G). Two or three macronuclei with single closely associated micronucleus (Figure 6D; Figure 7H, I). Locomotion by gliding between sand grains or along bottom of Petri dish.

Entire infraciliature consisting of dikinetids. Left lateral ciliary row extending around entire cell margin (Figure 6K; Figure 7K); 14–17 right lateral ciliary rows (Figure 6J; Figure 7O); dorsolateral kinety extending to posterior end of cell (Figure 6J; Figure 7L). Right buccal kinety longitudinal along right margin of buccal overture, composed of 75–105 tightly spaced dikinetids. Left outer buccal kinety longitudinal along left margin of buccal overture, composed of 15–25 closely spaced dikinetids. Intrabuccal kinety composed of 24–37 dikinetids (Figure 6E, F; Figure 7J, K, M).

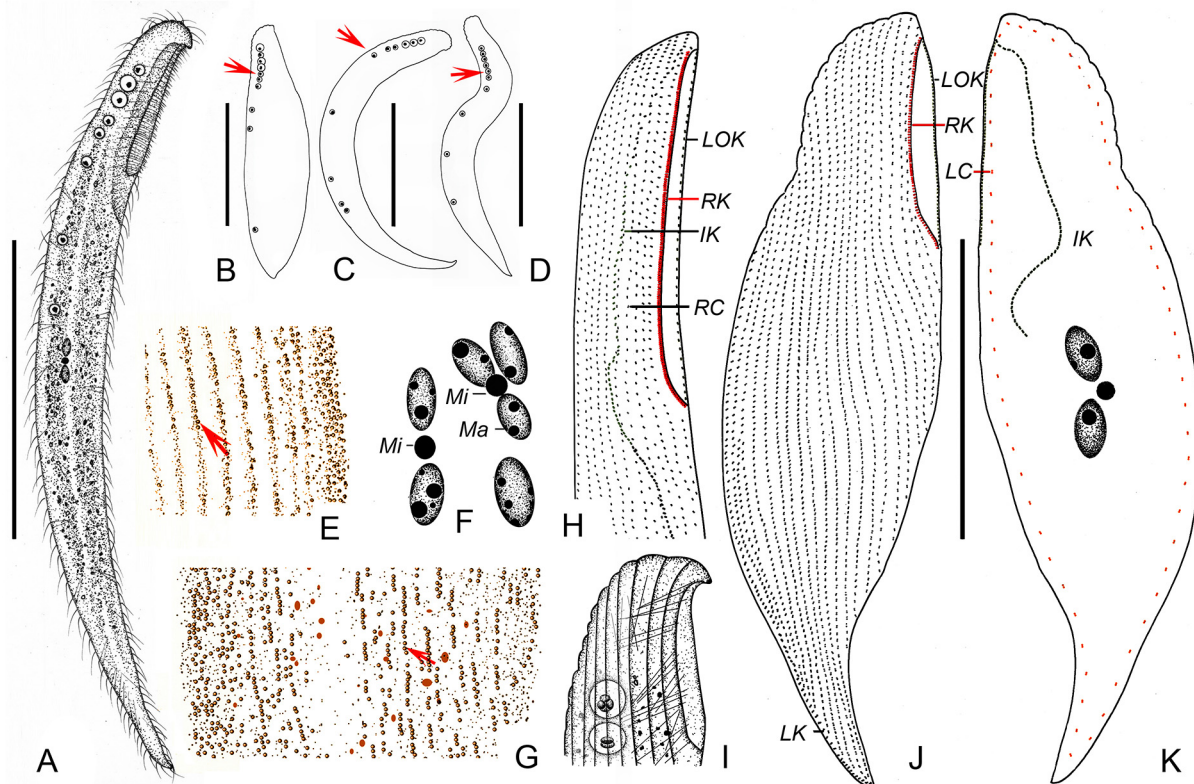


**Figure 4** *Remanella elongata* sp. nov. from life (A–G, I) and after protargol staining (H, J–K)

A: Typical individual. B–D: Different body shapes. Arrows point to Müller vesicles. E, G: Distribution of cortical granules (arrows) in right side (E) and left side (G). F: Variation in composition of nuclear group. H: Right side view of buccal infraciliature. I: Anterior region of right side. J, K: Infraciliature of right (J) and left (K) sides of holotype specimen, noting ciliary rows. IK, intrabuccal kinety; LOK, left outer buccal kinety; LC, left lateral ciliary row; LK, dorsolateral kinety; Ma, macronuclei; Mi, micronucleus; RC, right lateral ciliary rows; RK, right buccal kinety. Scale bars: 150  $\mu\text{m}$  (A–D); 100  $\mu\text{m}$  (J, K).

***Remanella unicorpusculata* (Kahl, 1933) stat. nov.**

**Synonyms:** *Remanella unicorpusculata* Dragesco, 1965

*Remanella rugosa* var. *aunicorpusculata* (Kahl, 1933) Foissner, 1996 (Figures 8, 9; Table 1)

This species was first reported by Kahl (1933), who provided a brief sketch and description of a single-Müller-vesicle variety of *Remanella rugosa*, named *Remanella rugosa* var. *unicorpusculata*. Later, Dragesco (1965) named it as *Remanella unicorpusculata*, with a description of body length, number of right lateral ciliary rows, and number of macronuclei. However, no information on its oral ciliature has been given. In addition, the genus *Remanella* was not valid until *R. multinucleata* (Kahl, 1933) Foissner, 1996 was fixed as the type species (Foissner, 1996). According to Foissner (1996), *Remanella unicorpusculata* was an invalid species due to a misinterpretation of the International Commission on Zoological Nomenclature (ICZN) in Dragesco (1965). Nevertheless, the established species from Dragesco (1965) can be clearly distinguished from *R. rugosa* by its single Müller vesicle and smaller body size. Therefore, in the present study, we elevate *Remanella rugosa* var. *unicorpusculata* to *Remanella unicorpusculata* (Kahl, 1933) stat. nov. and provide an improved diagnosis and a redescription based on present and previous studies.

**Improved diagnosis:** Cell size *in vivo* 90–140  $\mu\text{m}$  × 15–20  $\mu\text{m}$ ;

buccal field occupying ca. 15%–25% of body length; 7–10 right lateral ciliary rows; right buccal, left outer buccal, and intrabuccal kinety composed of 20–33, 3–5, and 9–20 dikinetids, respectively; 2–3 macronuclei; single micronucleus; brown cortical granules; one Müller vesicle. Marine habitat.

**Voucher slides:** Voucher slides of protargol-impregnated specimens from Qingdao population were deposited in the Laboratory of Protozoology, OUC, China (Registration No.: MMZ2020060801).

**Type locality, ecological features, and sample date:** Intertidal zone of First Bathing Beach at Qingdao (N36°03'24", E120°20'32"), China (Figure 1). Water temperature was 24 °C and salinity was ca. 30‰. Sample was collected on 8 June 2020.

**Description of population from China:** Live cells 90–140  $\mu\text{m}$  × 15–20  $\mu\text{m}$ , most about 110  $\mu\text{m}$  × 18  $\mu\text{m}$  in size, with buccal field occupying ca. 15%–25% of body length (Figure 8A; Figure 9A–D). Cilia about 10  $\mu\text{m}$  long. Cells rather transparent and almost colorless. Cell surface of left side rather rough, brown cortical granules sparsely scattered (Figure 8D; Figure 9E). One Müller vesicle, about 6  $\mu\text{m}$ –8  $\mu\text{m}$  in diameter with ellipsoidal mineral content, ca. 3  $\mu\text{m}$ –5  $\mu\text{m}$  in diameter, located near dorsal margin in anterior portion; 1–2 developing Müller vesicles present in middle region of posterior portion (Figure 8A–C; Figure 9A, B, F). Cytoplasmic spicules about 10

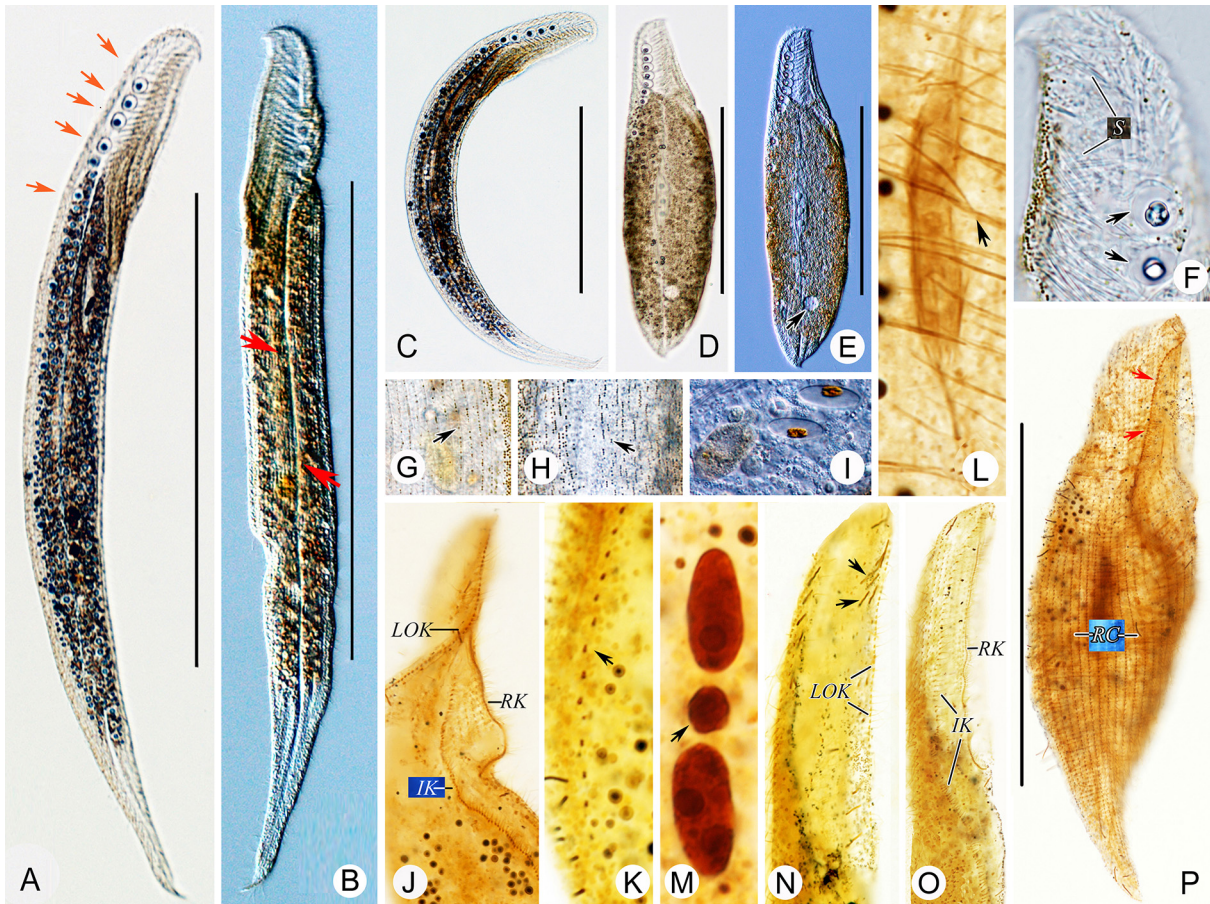


**Figure 5** *Remanella elongata* sp. nov. from life (A–I) and after protargol staining (J–P)

A–C: Typical individuals. Arrows in A point to Müller vesicles. Arrows in B show furrow on left side. D, E: Views of different contractive individuals, arrow points to vacuole. F: Anterior region. Arrows point to Müller vesicles. G, H: Distribution of cortical granules (arrows) in right side (G) and left side (H). I: Inclusions and granules. J: View of buccal infraciliature. K: Left lateral ciliary row (arrow). L: Nuclear groups. Arrow shows spicule. M: Nuclear groups. Arrow shows micronucleus. N, O: Oral infraciliature showing left outer buccal kinety (LOK), right buccal kinety (RK), and intrabuccal kinety (IK), arrows show spicules. P: Infraciliature of right side of holotype specimen. Arrows showing intrabuccal kinety. IK, intrabuccal kinety; LOK, left outer buccal kinety; Ma, macronuclei; RC, right lateral ciliary rows; RK, right buccal kinety; S, spicules. Scale bars: 300  $\mu$ m (A–C); 150  $\mu$ m (D, E, P).

$\mu$ m–15  $\mu$ m long, scattered throughout cell. Alga observed in body (Figure 9H, I). Two or three macronuclei with single micronucleus in-between (Figure 8E; Figure 9G, N, O).

Infraciliature consisting of dikinetids. Right surface densely ciliated, with 7–10 right lateral ciliary rows (Figure 8H; Figure 9P). Dorsolateral kinety extending to end of tail (Figure 8G; Figure 9M). Left lateral ciliary row curving around cell (Figure 8I; Figure 9Q). Right buccal kinety longitudinal along right margin of buccal overture, composed of 20–33 tightly spaced dikinetids (Figure 8F, H; Figure 9L, P). Left outer buccal kinety composed of 3–5 dikinetids. Intrabuccal kinety consisting of 9–20 dikinetids (Figure 8F, H, I; Figure 9J–L).

#### Molecular data and phylogenetic analyses

**Sequence information:** The sequence lengths of *Remanella rugosa*, *Remanella elongate* sp. nov., *Remanella aposinica* sp. nov., and *Remanella unicorpusculata* (Kahl, 1933) stat. nov. were 1 546, 1 547, 1 545, and 1 546 bp, respectively. The GC contents were 47.54%, 48.09%, 47.96%, and 47.80%,

respectively. GenBank accession Nos. of the four newly generated sequences were OM127343, OM127344, OM127345, and OM127342, respectively.

**Phylogenies inferred from SSU rDNA:** The ML and BI trees showed similar topologies and thus only the ML tree topology was presented (Figure 10). The family Loxodidae was well-supported as a monophyletic group (97% ML, 1.00 BI), forming a sister clade to the family Trachelocercidae (69% ML, 1.00 BI). *Remanella* formed a well-supported clade basal to the genus *Loxodes* in phylogenetic analyses. The hypothesis of the genus *Remanella* being monophyletic was rejected based on the AU test ( $P=0.017<0.05$ ). The four newly sequenced *Remanella* species were all contained within Loxodidae, as expected. *Remanella elongata* sp. nov. grouped with *R. caudata*, together clustering with the *Loxodes* species. The sequences of *R. rugosa* and *R. sp.* (JX015378) were identical, and thus they clustered together with full support. *Remanella elongate* sp. nov. and *R. caudata* grouped together with weak support, with a 71 bp difference



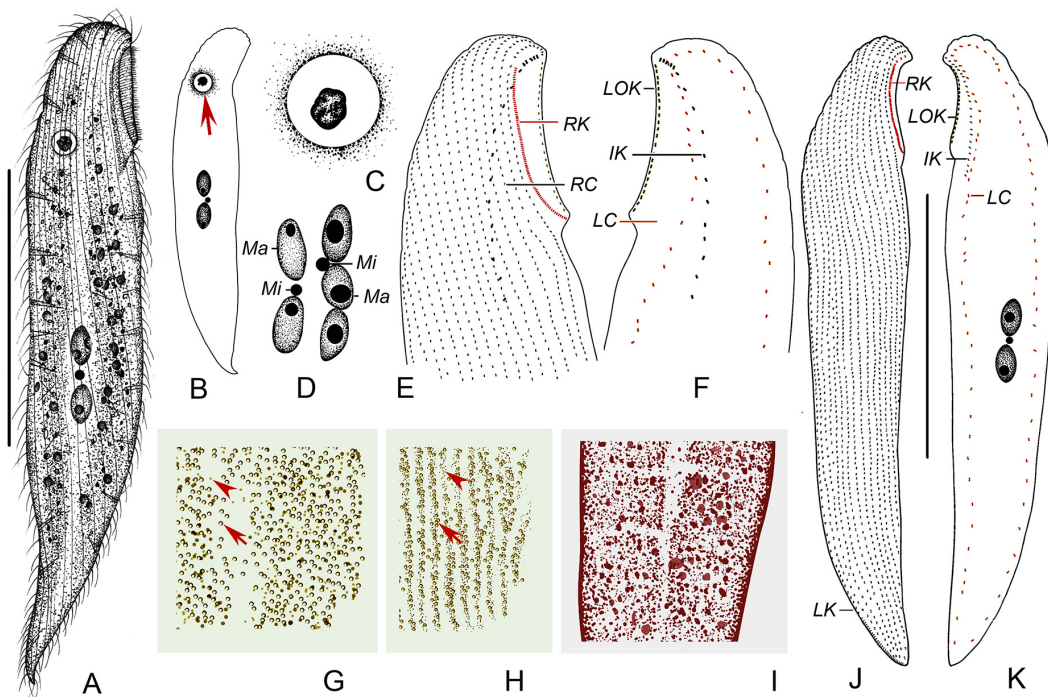


**Figure 6** *Remanella aposinica* sp. nov. from life (A–D, G–I) and after protargol staining (E–F, J–K)

A: Typical individual. B: Different body shape. Arrow points to Müller vesicle. C: Müller vesicle. D: Variation in composition of nuclear group. E, F: Right (E) and left (F) side view of buccal infraciliature. G, H: Distribution of cortical granules (arrows) in right side (H) and left side (G). Arrowheads point to granules in cytoplasm. I: Cell surface of left side rather rough due to many wrinkles. J, K: Infraciliature of right (J) and left (K) sides of holotype specimen, noting ciliary rows. IK, intrabuccal kinety; LOK, left outer buccal kinety; LC, left lateral ciliary row; LK, dorsolateral kinety; RC, right lateral ciliary rows; RK, right buccal kinety. Scale bars: 150  $\mu$ m (A, J, K).

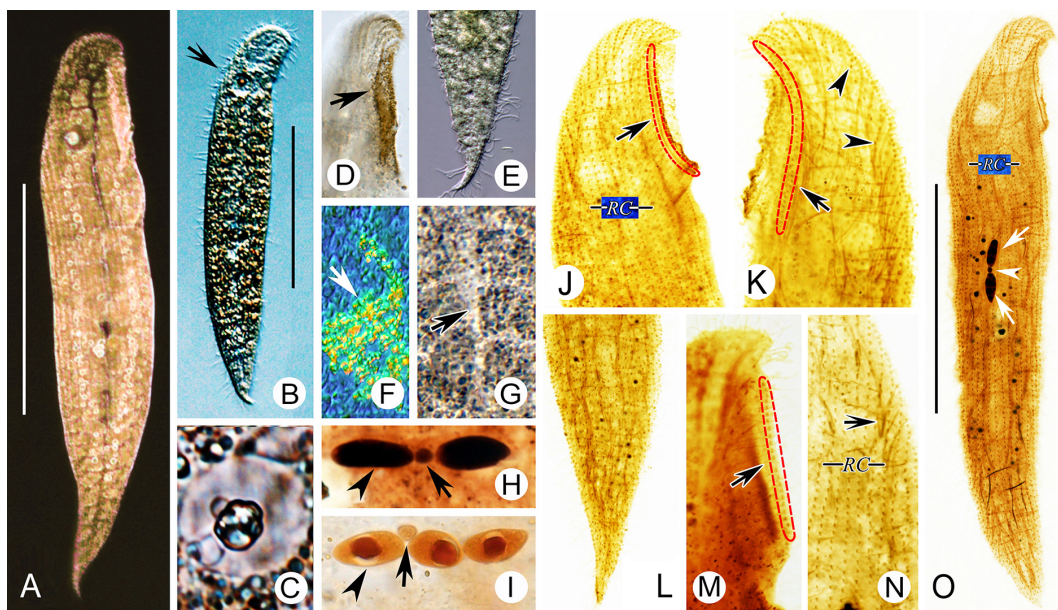


**Figure 7** *Remanella aposinica* sp. nov. from life (A–G) and after protargol staining (H–O)

A, B: Typical individuals. Invertible function in Photoshop. Arrow shows Müller vesicle. C: Müller vesicle. D: Distribution of cortical granules of buccal region (arrow). E: Posterior of cell. F: Inclusions and granules (arrow). G: Left side. Arrows show wrinkles. H, I: Nuclear groups. Arrowheads point to macronuclei. Arrows show micronuclei. J: Right side of anterior region. Arrow shows right buccal kinety. K: Arrow shows intrabuccal kinety. Arrowheads point to left lateral ciliary row. L: Posterior region. M: Arrow shows left outer buccal kinety. N: Part of right side. Arrow shows spicule. O: Infraciliature of right side of holotype specimen. Arrows show macronuclei. Arrowhead shows micronuclei. RC, right lateral ciliary rows. Scale bars: 150  $\mu$ m (A, B, O).

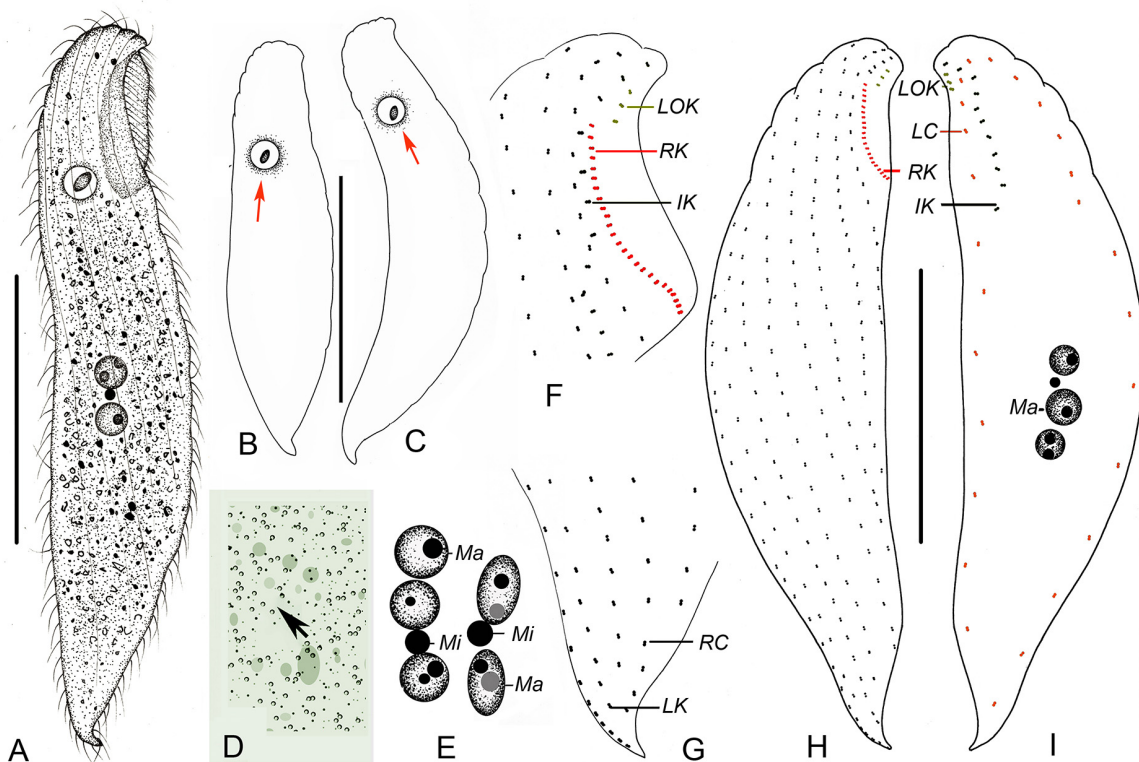


**Figure 8** *Remanella unicorpusculata* (Kahl, 1933) stat. nov. from life (A–E) and after protargol staining (F–I)

A: Representative individual. B, C: Different body shapes. Arrows point to Müller vesicles. D: Distribution of cortical granules (arrows) on left side. E: Variation in composition of nuclear group. F: Right side view of buccal infraciliature. G: Infraciliature of right posterior region. H, I: Infraciliature of right (H) and left (I) sides of specimen. IK, intrabuccal kinety; LOK, left outer buccal kinety; LC, left lateral ciliary row; LK, dorsolateral kinety; Ma, macronuclei; Mi, micronucleus; RC, right lateral ciliary rows; RK, right buccal kinety. Scale bars: 50  $\mu$ m (A–C, H, I).

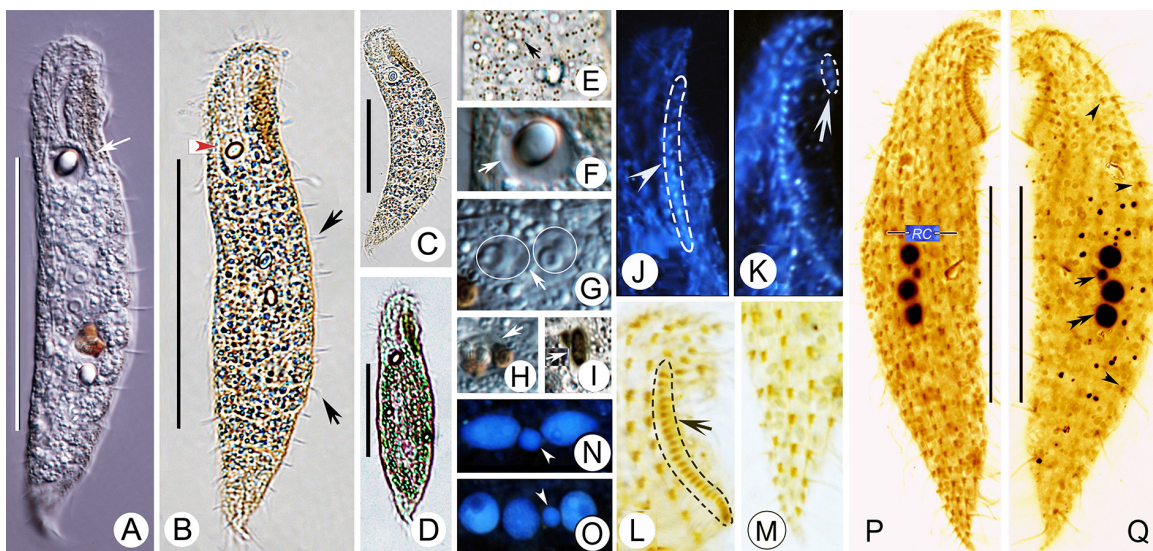


**Figure 9** *Remanella unicorpusculata* (Kahl, 1933) stat. nov. from life (A–I) and after protargol staining (J–Q)

A, B: Typical individuals. Arrow in A shows single Müller vesicle. Arrows in B show left lateral ciliary. Arrowhead (B) points to Müller vesicles. C, D: Views of different individuals. E: Distribution of cortical granules (arrow) on left side. F: Arrow points to Müller vesicle. G: Details of nuclear group. H, I: Inclusions and granules. J–L: Oral infraciliature showing intrabuccal kinety (J), left outer buccal kinety (K), and right buccal kinety (L). M: Posterior region of right side. N, O: Nuclear groups by invertible function in Photoshop. Arrowheads point to micronuclei. P, Q: Infraciliature of right (P) and left (Q) sides of specimen. Arrow shows micronucleus; double arrowheads show macronucleus; arrowheads show left lateral ciliary row. RC, right lateral ciliary rows. Scale bars: 80  $\mu$ m (A, B); 60  $\mu$ m (C, D); 50  $\mu$ m (P, Q).

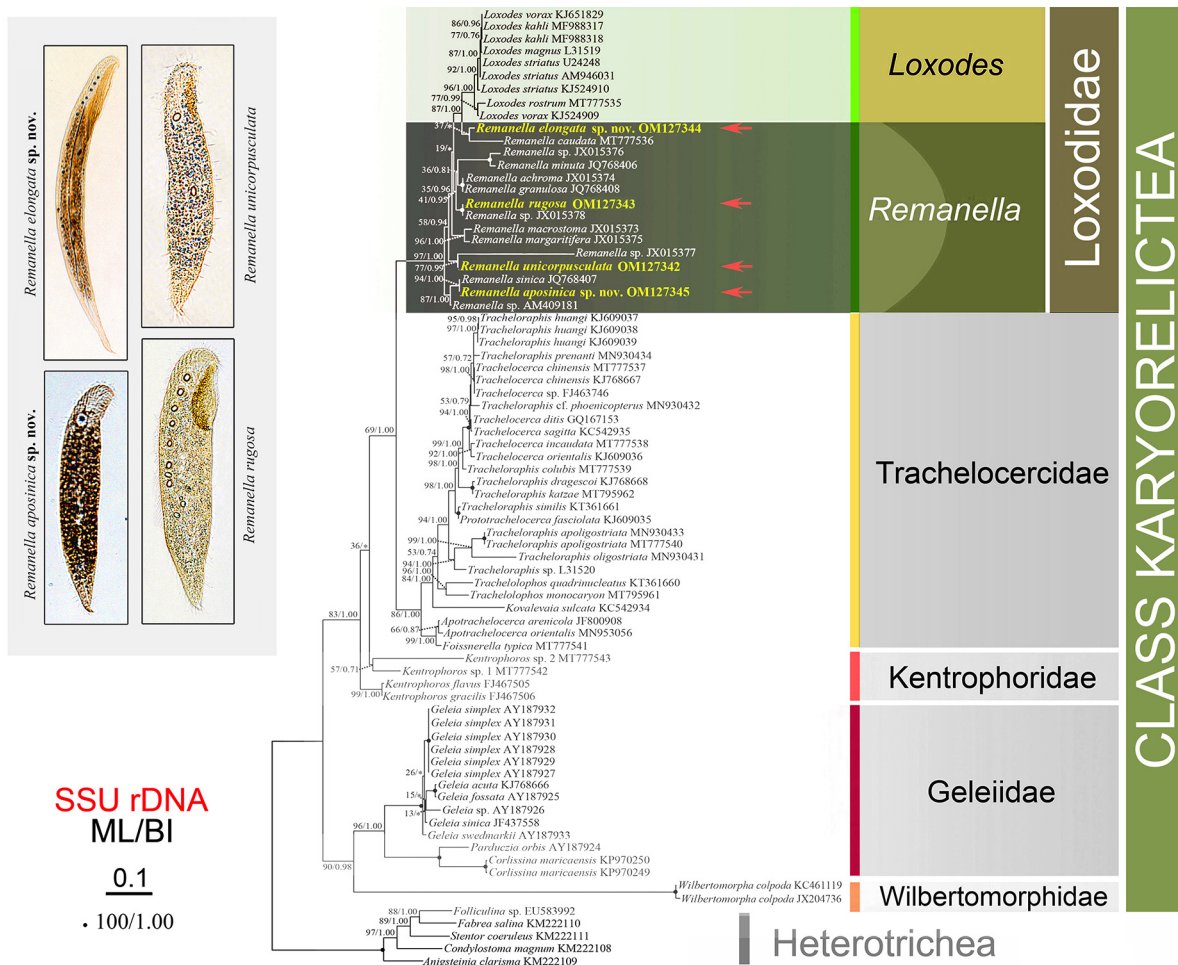


**Figure 10** ML tree inferred from SSU rDNA sequences showing phylogenetic positions of four newly sequenced species. Numbers near nodes represent ML bootstrap support and BI posterior probability values. Fully supported (100%/1.00) branches are marked with solid circles. Asterisks indicate disagreement between ML and BI trees. Sequences newly obtained are in bold. Scale bar corresponds to 10 substitutions per 100 nucleotide positions.

between in their sequences. *Remanella unicorpusculata* stat. nov. branched with *Remanella* sp. (JX015377), with a 182 bp difference between their sequences (Supplementary Table S1). *Remanella aposinica* sp. nov. clustered with *R. sinica* with strong support (94% ML, 1.00 BI) and a 6 bp difference, then together grouped with *Remanella* sp. (AM409181), forming an early-branching lineage with Loxodidae.

## DISCUSSION

### Comments on *Remanella rugosa* (kahl, 1933) Foissner, 1996

*Remanella rugosa* was originally described by Kahl (1933) as “Size 200–300  $\mu\text{m}$ , two elongated nuclei...Müller vesicles 3 to 8 ...” (translated from German). Considering the general morphology, the Chinese population corresponds well with the original description (Figure 2E). The main difference between the two populations is body size (200  $\mu\text{m}$ –300  $\mu\text{m}$  in the original population vs. usually 90  $\mu\text{m}$ –200  $\mu\text{m}$  in the Chinese population). However, this difference may be due to its

contractility. Therefore, the Chinese population is recognized as a new population of *R. rugosa*.

The species was later reported with more or fewer details in many places (Carey & Maeda, 1985; Dragesco, 1960; Hartwig, 1973; Kattar, 1970; Lepsi, 1962; Raikov, 1993). However, its infraciliature was not reported until Foissner (1996) but only by means of a figure and without a full redescription or morphometric data. Most other populations are similar to the Chinese population, except for the following. The population described by Dragesco (1960) has a larger body size range (180  $\mu\text{m}$ –400  $\mu\text{m}$  vs. 90  $\mu\text{m}$ –200  $\mu\text{m}$ ) and higher number of right lateral ciliary rows than the Chinese population (14–15 vs. 12–14). The sketch in Foissner (1996) also shows one left inner buccal kinety near the left outer buccal kinety. However, as there is no additional description of the sketch, the identification of this population should be further considered.

*Remanella rugosa* is similar to *R. brunnea* but differs by buccal to body length ratio (1/5–1/3 in *R. rugosa* vs. 1/9–1/5 in *R. brunnea*) (Dragesco, 1965).

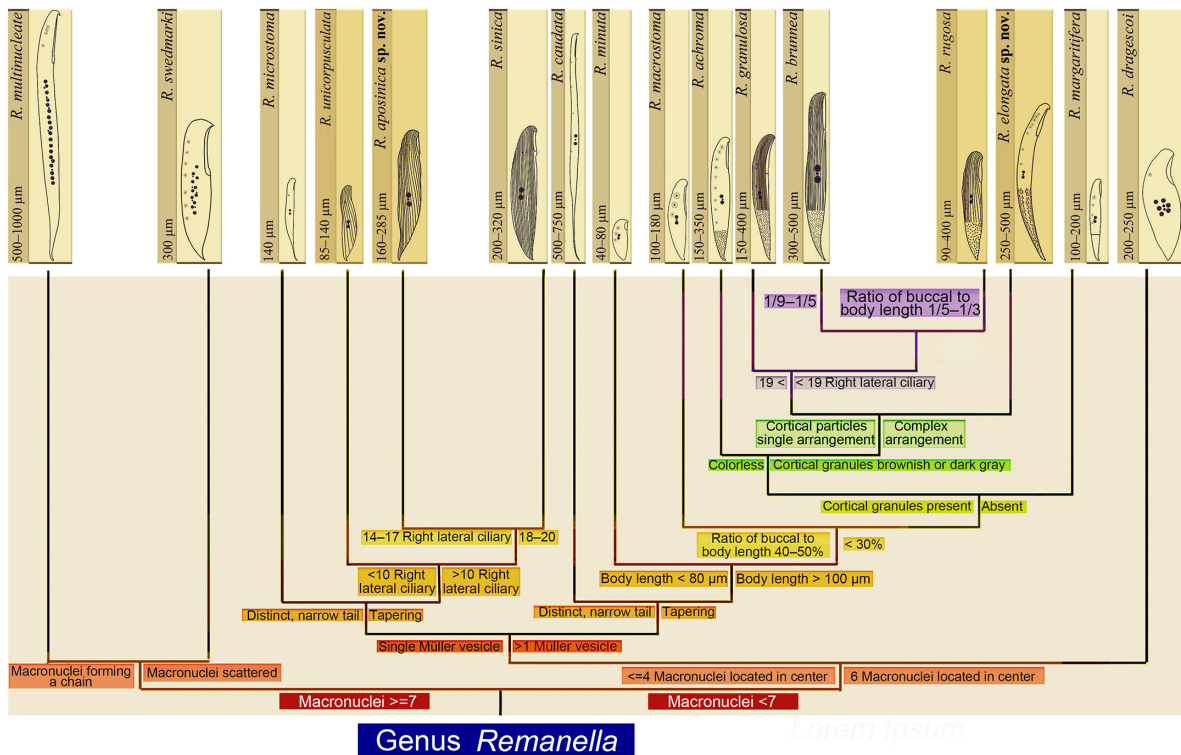


Figure 11 Illustration of updated identification key of 16 current species within *Remanella*

**Comments on *Remanella elongata* sp. nov.**

Considering the general morphology, including body shape, number of macronuclei, right lateral kineties, right buccal, left outer buccal, intrabuccal kinety, and color of cortical granules, *Remanella granulosa* (Kahl, 1933) Foissner, 1996 and *Remanella multinucleata* (Kahl, 1933) Foissner, 1996 should be compared with *Remanella elongata* sp. nov. (Figure 11 and Table 2).

*Remanella granulosa* differs from *Remanella elongata* sp. nov. by having sparsely scattered cortical granules in glabrous stripe (Xu et al., 2012) vs. cortical granules arranged in lines on both sides of glabrous stripe, sparse in middle of glabrous stripe, appearing as longitudinal bright “line” when observed *in vivo* (Figure 4G; Figure 5H).

*Remanella multinucleata* can be distinguished from *Remanella elongata* sp. nov. by longer body size (500 µm–1 000 µm vs. 250 µm–500 µm *in vivo*), different color and arrangement of cortical granules (yellowish, in rows vs. brown, complex arrangement), and more macronuclei (7–24 vs. 1–3).

**Comments on *Remanella aposinica* sp. nov.**

*Remanella aposinica* sp. nov. is mainly characterized by having one Müller vesicle. Considering this feature, *R. sinica* Xu et al., 2012, *R. unicorpusculata* Foissner, 1996, *R. dragescoi* (Agamaliyev, 1966) Foissner, 1996, and *R. microstoma* (Dragesco, 1954) Foissner, 1996 should be compared with the new species (Figure 11). *Remanella sinica* is similar to *Remanella aposinica* sp. nov. in general morphology *in vivo* and by having a single Müller vesicle (Table 2) but can be distinguished by having more right lateral ciliary rows (18–20 vs. 14–17). In addition, their SSU rDNA

sequences differ by 6 bp, indicating that these two organisms are not conspecific (Xu et al., 2012).

*Remanella unicorpusculata* differs from *Remanella aposinica* sp. nov. by its smaller size (90 µm–140 µm vs. 160 µm–285 µm) and fewer right lateral ciliary rows (7–10 vs. 14–17) (Dragesco, 1965; Table 2).

There is no information on the infraciliature of *R. dragescoi*. However, from the original report, it can be inferred that *R. dragescoi* differs from *Remanella aposinica* sp. nov. by having more macronuclei (6 vs. 2–3) (Agamaliyev, 1966).

Information on the infraciliature of *R. microstoma* is also lacking. Nevertheless, this species can be easily distinguished from *Remanella aposinica* sp. nov. by its distinct and narrow tail (ca. 1/4 of body length vs. short and inconspicuous), smaller body size (140 µm vs. 160 µm–285 µm), and smaller buccal field/body length ratio (1/7 vs. 1/6–1/5) (Dragesco, 1954b).

**Comments on *Remanella unicorpusculata* (Kahl, 1933) stat. nov.**

*Remanella unicorpusculata* (Kahl, 1933) stat. nov. is characterized by one Müller vesicle and smaller body size. According to Xu et al. (2013a), the number of Müller vesicles is an important character for identifying species in Loxodidae. Considering the differences in Müller vesicle numbers between *R. rugosa unicorpusculata* (Kahl, 1933) Foissner, 1996 and *R. rugosa* (1 vs. 3–8), we agree with Dragesco (1965) on elevating this species to species-rank, *Remanella unicorpusculata* (Kahl, 1933) stat. nov. (Table 2). Furthermore, our population corresponds well with the original description and that of Dragesco (1965), i.e., “85–100 µm

**Table 2 Morphometric comparison between nominal species of *Remanella* (µm)**

Species	Body length, µm, <i>in vivo</i>	Buccal field/body length (based on specimens <i>in vivo</i> )	RC, No (after staining)	LOK, No. (after staining)	IK, No. (after staining)	RK, No. (after staining)	Ma, No. (after staining)	M, No. (based on specimens <i>in vivo</i> )	Color of cortical granules (based on specimens <i>in vivo</i> )	Cortical granules arrangement (based on specimens <i>in vivo</i> )	Data source
<i>Remanella rugosa</i>	90–400	1/5–1/3	11–15	14–25	23–40	40–60	2–3	3–10	Brown	Scattered	This study; Carey & Maeda, 1985; Dragesco, 1960; Kattar, 1970; Raikov, 1993
<i>Remanella elongata</i> sp. nov.	250–500	1/4–1/3	18–22	50–100	105–150	125–180	1–3	7–13	Brown	In rows and scattered	This study
<i>Remanella aposinica</i> sp. nov.	160–285	1/6–1/5	14–17	15–25	24–37	75–105	2–3	1	Brown	Scattered	This study
<i>Remanella unicolorpusculata</i> (Foissner, 1996) stat. nov.	90–140	15%–25%	7–10	3–5	9–20	20–33	2–3	1	Brown	Scattered	This study; Dragesco, 1965
<i>R. multinucleata</i>	500–1 000	1/5–1/4	18–27	43–140	75–135	–	7–24	1–4	Yellow	In rows	Foissner, 1996
<i>R. swedmarki</i>	300–350	ca. 1/3 <sup>a</sup>	20–30	ca. 58 <sup>b</sup>	–	ca. 100 <sup>b</sup>	11–60	6 <sup>b</sup>	Brown	–	Dragesco, 1954a, 1963
<i>R. dragescoi</i>	200–250	ca. 1/5–1/4 <sup>a</sup>	20	–	–	–	6	1	–	–	Agamaliev, 1966
<i>R. microstoma</i>	140	ca. 1/7 <sup>a</sup>	–	–	–	–	2 <sup>b</sup>	1 <sup>b</sup>	Absent	Absent	Dragesco, 1954b
<i>R. caudata</i>	500–750	ca. 1/8 <sup>a</sup>	–	–	–	–	2	4 <sup>b</sup>	–	–	Dragesco, 1954b, 1960
<i>R. sinica</i>	200–320	ca. 1/6–1/5	18–20	15–27	39–47	69–84	1–3	1	Brown	Scattered	Xu et al., 2012
<i>R. minuta</i>	40–80	ca. 1/4	12–14	7–10	22–29	37–56	2	ca. 3–4	Brown	Scattered	Xu et al., 2012
<i>R. macrostoma</i>	100–180	ca. 40%–50%	10–15	18–46	22–52	50–99	2–4	ca. 3–4	Dark gray to brown	Scattered	Xu et al., 2013a
<i>R. margaritifera</i>	100–200	ca. 18%–25%	9–11	8–14	15–25	17–37	1–2	ca. 3–4	Absent	Absent	Xu et al., 2013a
<i>R. achroma</i>	150–350	ca. 1/4	17–24	24–53	31–60	71–133	2–3	ca. 6–8	Colorless	Scattered	Xu et al., 2013a
<i>R. granulosa</i>	150–400	ca. 1/5–1/4	19–23	35–70	64–78	140–189	2–3	8–9	Brown	Scattered	Xu et al., 2012
<i>R. brunnea</i>	300–500	ca. 1/9–1/5 <sup>a</sup>	15–16	–	–	–	2	6–12	Brown	Scattered	Dragesco, 1965

M: Müller vesicles; Ma: Macronuclei; RC: Right lateral ciliary rows; RK: Right buccal kinety; IK: Intrabuccal kinety; LOK: Left outer buccal kinety; –: Data not available.

long, one Müller vesicles, ten right lateral ciliary rows, brown cortical granules, two macronuclei and one micronucleus...".

Similar to the comparisons for *Remanella aposinica* sp. nov. classification, *Remanella unicorpusculata* (Kahl, 1933) stat. nov. should also be compared with *R. sinica* Xu et al., 2012, *R. dragescoi* (Agamaliyev, 1966) Foissner, 1996, and *R. microstoma* (Dragesco, 1954) Foissner, 1996, which are all characterized by single Müller vesicles.

*Remanella sinica* differs from *Remanella unicorpusculata* (Kahl, 1933) stat. nov. based on its larger size (200 µm–320 µm vs. 90 µm–140 µm) and more right lateral ciliary rows (18–20 vs. 7–10) (Xu et al., 2012).

From its original description, *R. dragescoi* differs from *Remanella unicorpusculata* (Kahl, 1933) stat. nov. by having more macronuclei (6 vs. 2–3) (Agamaliyev, 1966).

With its distinct features, *R. microstoma* can be distinguished from *Remanella unicorpusculata* (Kahl, 1933) stat. nov. based on its narrow tail (ca. 1/4 of body length vs. short and wedge-shaped (Dragesco, 1954b).

### Comments on phylogenetic analyses

The class Karyorelictea is a stable monophyletic group, as reported previously (Ma et al., 2022; Xu et al., 2012, 2013a). The class can be subdivided into five families: Loxodidae, Geleidae, Kentrophoridae, Wilbertomorphidae, and Trachelocercidae. Loxodidae and Trachelocercidae have a close relationship. Within Loxodidae, *Loxodes* is located within *Remanella*, well reflecting previous reports that freshwater *Loxodes* is likely to have evolved from marine *Remanella* (Xu et al., 2013a). *Remanella unicorpusculata*, *R. sinica*, *R. aposinica*, and the other two *Remanella* sp. form the two early branches. In addition, single Müller vesicles may be an ancestral character.

### Identification key of genus *Remanella*

Based on previous studies and our present work, an updated key to the identification of species within the genus *Remanella* is provided (Figure 11):

- 1) Macronuclei seven or more, forming chain or scattered in cell ..... 2
- 1.1) Macronuclei six or less, located in center of cell ..... 3
- 2) Macronuclei seven to 27, forming chain in central third of cell ..... *R. multinucleata*
- 2.1) Macronuclei 11 to 60, scattered in cell ..... *R. swedmarki*
- 3) Macronuclei six, located in center of cell ..... *R. dragescoi*
- 3.1) Macronuclei less than four, located in center of cell ..... 4
- 4) Müller vesicle always single ..... 5
- 4.1) Müller vesicle more than one ..... 8
- 5) Posterior part forming distinct, narrow tail ... *R. microstoma*
- 5.1) Posterior part tapering ..... 6
- 6) Right lateral ciliary rows less than 10 ... *R. unicorpusculata*
- 6.1) Right lateral ciliary rows more than 10 right lateral ciliary rows ..... 7
- 7) Right lateral ciliary rows 14–17.....  
..... *Remanella aposinica* sp. nov.
- 7.1) Right lateral ciliary rows 18–20 ..... *R. sinica*
- 8) Posterior part forming a distinct, narrow tail ..... *R. caudata*
- 8.1) Posterior part tapering ..... 9
- 9) Body length *in vivo* smaller than 80 µm ..... *R. minuta*

- 9.1) Body length *in vivo* longer than 100 µm ..... 10
- 10) Ratio of buccal field to body length of 40%–50% .....  
..... *R. macrostoma*
- 10.1) Ratio of buccal field to body length smaller than 30%....  
..... 11
- 11) Cortical granules absent ..... *R. margaritifera*
- 11.1) Cortical granules present ..... 12
- 12) Cortical granules colorless ..... *R. achroma*
- 12.1) Cortical granules brown or dark gray ..... 13
- 13) Cortical particles single arrangement ..... 14
- 13.1) Cortical particles complex arrangement .....  
..... *Remanella elongata* sp. nov.
- 14) Right lateral ciliary rows more than 19 ..... *R. granulosa*
- 14.1) Right lateral ciliary rows less than 19 ..... 15
- 15) Ratio of buccal to body length 1/5–1/3 ..... *R. rugosa*
- 15.1) Ratio of buccal to body length 1/9–1/5 ..... *R. brunnea*

### NOMENCLATURAL ACTS REGISTRATION

The electronic version of this article in portable document format will represent a published work according to the International Commission on Zoological Nomenclature (ICZN), and hence the new names contained in the electronic version are effectively published under that Code from the electronic edition alone (see Article 8.5–8.6 of the Code). This published work and the nomenclatural acts it contains have been registered in ZooBank, the online registration system for ICZN. The ZooBank LSIDs (Life Science Identifiers) can be resolved and the associated information can be viewed through any standard web browser by appending the LSID to prefix <http://zoobank.org/>.

Publication LSID:

urn:lsid:zoobank.org:pub:1ACD9A93-8BB0-454E-91B7-6CCF ECD396C0

Nomenclatural act LSID:

*Remanella elongata* sp. nov. urn:lsid:zoobank.org:act:62EB 1882-EAF3-4BD5-8516-402903DEAD5D

*Remanella aposinica* sp. nov. urn:lsid:zoobank.org:act:28E 326F3-6BBC-4AA9-B00E-EF7B68DA45CF

### AUTHOR CONTRIBUTIONS

M.Z.M. and Y.J.L. performed the experiments and data analyses. M.Z.M. wrote the original draft. Y.X., B.R.L., Y.Q.L., S.A.A., G.P., W.B.S., and Y.Y. reviewed and edited the manuscript. All authors read and approved the final version of the manuscript.

### ACKNOWLEDGEMENTS

Many thanks are due to Dr. Zhe Wang (Shandong University) for his help with topology testing.

### REFERENCES

- Agamaliyev FG. 1966. New species of psammobiotic ciliates of the western coast of the Caspian Sea. *Acta Protozoologica*, 4: 169–184 (in Russian)
- Andreoli I, Mangini L, Ferrantini F, Santangelo G, Verni F, Petroni G. 2009. Molecular phylogeny of unculturable Karyorelictea (Alveolata, Ciliophora). *Zoologica Scripta*, 38(6): 651–662.

- Carey PG, Maeda M. 1985. Horizontal distribution of psammophilic ciliates in fine sediments of the Chichester Harbour area. *Journal of Natural History*, **19**(3): 555–574.
- Dragesco J. 1954a. Diagnoses préliminaires de quelques ciliés psammophiles nouveaux. *Bulletin de la Société Zoologique de France, Paris*, **79**: 57–62.
- Dragesco J. 1954b. Diagnoses préliminaires de quelques ciliés nouveaux des sables de Banyuls-Sur-Mer (I). *Vie Milieu*, **4**(4): 633–637.
- Dragesco J. 1960. Ciliés mésopsammiques littoraux. Systématique, morphologie, écologie. *Des Travaux De La Station Biologique de Roscoff (N. S.)*, **12**: 1–356.
- Dragesco J. 1963. Compléments à la connaissance des ciliés mésopsammiques de Roscoff. I. Holotriches. *Cahiers De Biologie Marine*, **4**(3): 91–119.
- Dragesco J. 1965. Ciliés mésopsammiques d'Afrique noire. *Cahiers De Biologie Marine*, **6**(4): 357–399.
- Fenchel T, Finlay BJ. 1986. The structure and function of Müller vesicles in loxodid ciliates. *The Journal of Protozoology*, **33**(1): 69–76.
- Foissner W. 1996. A redescription of *Remanella multinucleata* (Kahl, 1933) nov. gen., nov. comb. (Ciliophora, Karyorelictea), emphasizing the infraciliature and extrusomes. *European Journal of Protistology*, **32**(2): 234–250.
- Foissner W. 1998. The karyorelictids (Protozoa: Ciliophora), a unique and enigmatic assemblage of marine, interstitial ciliates: a review emphasizing ciliary patterns and evolution. In: Coombs GH, Vickerman K, Sleight MA, Warren A. *Evolutionary Relationships Among Protozoa*. London: Chapman & Hall, 305–325.
- Gao S, Strüder-Kypke MC, Al-Rasheid KAS, Lin XF, Song WB. 2010. Molecular phylogeny of three ambiguous ciliate genera: *Kentrophoros*, *Trachelolophos* and *Trachelotractus* (Alveolata, Ciliophora). *Zoologica Scripta*, **39**(3): 305–313.
- Hall TA. 1999. BioEdit: a user-friendly biological sequence alignment editor and analysis program for Windows 95/98/NT. *Nucleic Acids Symposium Series*, **41**: 95–98.
- Hartwig E. 1973. Die Ciliaten des Gezeiten-Sandstrandes der Nordseeinsel Sylt. I. *Systematik. Mikrofauna Meeresboden*, **18**: 385–453.
- Hu XZ, Lin XF, Song WB. 2019. *Ciliate Atlas: Species Found in the South China Sea*. Beijing: Science Press.
- Jerome CA, Lynn DH, Simon EM. 1996. Description of *Tetrahymena empidokyrea* n. sp., a new species in the *Tetrahymena pyriformis* sibling species complex (Ciliophora, Oligohymenophorea), and an assessment of its phylogenetic position using small-subunit rRNA sequences. *Canadian Journal of Zoology*, **74**(10): 1898–1906.
- Kahl A. 1933. Ciliata libera et ectocommensalia. In: Grimpe G, Wagler E. *Die Tierwelt der Nord-und Ostsee*, Vol. 23. Leipzig: Akademische Verlagsgesellschaft, 29–146.
- Kattar MR. 1970. Estudo dos protozoários ciliados psamófilos do litoral brasileiro. *Boletim de Zoologia e Biologia Marinha*, **27**(27): 123–206.
- Lepsi I. 1962. Über einige insbesondere psammobionte Ciliaten vom rumänischen Schwarzmeer-Ufer. *Zoologischer Anzeiger*, **168**: 460–465.
- Lynn DH. 2008. *The Ciliated Protozoa: Characterization, Classification, and Guide to the Literature*. 3<sup>rd</sup> ed. New York: Springer.
- Ma MZ, Li YQ, Ma HG, Al-Rasheid KAS, Warren A, Wang YR, et al. 2021a. Morphology and molecular phylogeny of four Trachelocercid Ciliates (Protozoa, Ciliophora, Karyorelictea) found in Marine Coastal Habitats of Northern China, with Description of a New Genus, two new species and a new combination. *Frontiers in Marine Sciences*, **7**: 615903.
- Ma MZ, Li YQ, Maurer-Alcalá XX, Wang YR, Yan Y. 2022. Deciphering phylogenetic relationships in class Karyorelictea (Protista, Ciliophora) based on updated multi-gene information with establishment of a new order Wilbertomorphida n. ord. *Molecular Phylogenetics and Evolution*, **169**: 107406.
- Ma MZ, Xu Y, Yan Y, Li YQ, Warren A, Song WB. 2021b. Taxonomy and molecular phylogeny of four karyorelictid species belonging to the genera *Apotrachelocerca* and *Tracheloraphis* (Protozoa: Ciliophora), with descriptions of two new species. *Zoological Journal of the Linnean Society*, **192**(3): 690–709.
- Mazei Y, Gao S, Warren A, Li L, Li J, Song W, et al. 2009. A reinvestigation of the marine ciliate *Trachelocerca ditis* (Wright, 1982) Foissner and Dragesco, 1996 (Ciliophora, Karyorelictea) from the Yellow Sea and an assessment of its phylogenetic position inferred from the small subunit rRNA gene sequence. *Acta Protozoologica*, **48**(3): 213–221.
- Medlin L, Elwood HJ, Stickel S, Sogin ML. 1988. The characterization of enzymatically amplified eukaryotic 16S-like rRNA-coding regions. *Gene*, **71**(2): 491–499.
- Nylander JAA. 2004. MrModeltest, Version 2. Program Distributed by the Author. Uppsala: Evolutionary Biology Centre, Uppsala University.
- Penn O, Privman E, Ashkenazy H, Landan G, Graur D, Pupko T. 2010. GUIDANCE: a web server for assessing alignment confidence scores. *Nucleic Acids Research*, **38**(S2): W23–W28.
- Raikov IB. 1993. The orthonematocyst, a new type of extrusome found in *Remanella rugosa* and *Remanella brunnea* (Ciliophora: Karyorelictida). *European Journal of Protistology*, **29**(1): 81–87.
- Ronquist F, Teslenko M, Van Der Mark P, Ayres DL, Darling A, Höhna S, et al. 2012. MrBayes 3.2: efficient Bayesian phylogenetic inference and model choice across a large model space. *Systematic Biology*, **61**(3): 539–542.
- Shimodaira H. 2002. An approximately unbiased test of phylogenetic tree selection. *Systematic Biology*, **51**(3): 492–508.
- Shimodaira H, Hasegawa M. 2001. CONSEL: for assessing the confidence of phylogenetic tree selection. *Bioinformatics*, **17**(12): 1246–1247.
- Song WB, Warren A, Hu XZ. 2009. *Free-Living Ciliates in the Bohai and Yellow Seas*. Beijing: Science Press. (in Chinese)
- Stamatakis A. 2014. RAxML version 8: a tool for phylogenetic analysis and post-analysis of large phylogenies. *Bioinformatics*, **30**(9): 1312–1313.
- Stamatakis A, Hoover P, Rougemont J. 2008. A rapid bootstrap algorithm for the RAxML web servers. *Systematic Biology*, **57**(5): 758–771.
- Tamura K, Peterson D, Peterson N, Stecher G, Nei M, Kumar S. 2011. MEGA5: molecular evolutionary genetics analysis using maximum likelihood, evolutionary distance, and maximum parsimony methods. *Molecular Biology and Evolution*, **28**(10): 2731–2739.
- Wang L, Qu Z S, Li S, Hu X Z. 2019a. Morphology and molecular phylogeny of two little-known species of *Loxodes*, *L. kahli* Dragesco & Njiné, 1971 and *L. rostrum* Müller, 1786 (Protist, Ciliophora, Karyorelictea). *Journal of Ocean University of China*, **18**(3): 643–653.
- Wang YR, Jiang YH, Liu YQ, Li Y, Katz LA, Gao F, et al. 2020. Comparative studies on the polymorphism and copy number variation of mtSSU rDNA in ciliates (Protista, Ciliophora): implications for phylogenetic, environmental, and ecological research. *Microorganisms*, **8**(3): 316.
- Wang YR, Wang CD, Jiang YH, Katz LA, Gao F, Yan Y. 2019b. Further analyses of variation of ribosome DNA copy number and polymorphism in ciliates provide insights relevant to studies of both molecular ecology and phylogeny. *Science China Life Sciences*, **62**(2): 203–214.

- Wilbert N. 1975. Eine verbesserte Technik der Protargolimprägung für Ciliaten. *Mikrokosmos*, **64**: 171–179.
- Xu Y, Gao S, Hu XZ, Al-Rasheid KAS, Song WB. 2013a. Phylogeny and systematic revision of the karyorelictid genus *Remanella* (Ciliophora, Karyorelictea) with descriptions of two new species. *European Journal of Protistology*, **49**(3): 438–452.
- Xu Y, Li JM, Song WB, Warren A. 2013b. Phylogeny and establishment of a new ciliate family, Wilbertomorphidae fam. nov. (Ciliophora, Karyorelictea), a highly specialized taxon represented by *Wilbertomorpha colpoda* gen. nov., spec. nov. *Journal of Eukaryotic Microbiology*, **60**(5): 480–489.
- Xu Y, Miao M, Warren A, Song WB. 2012. Diversity of the karyorelictid ciliates: *Remanella* (Protozoa, Ciliophora, Karyorelictida) inhabiting intertidal areas of Qingdao, China, with descriptions of three species. *Systematics and Biodiversity*, **10**(2): 207–219.
- Yan Y, Gao F, Xu Y, Al-Rasheid KAS, Song WB. 2015. Morphology and phylogeny of three trachelocercid ciliates, with description of a new species, *Trachelocerca orientalis* spec. nov. (Ciliophora, Karyorelictea). *Journal of Eukaryotic Microbiology*, **62**(2): 157–166.
- Yan Y, Maurer-Alcalá XX, Knight R, Pond SLK, Katz LA. 2019. Single-cell transcriptomics reveal a correlation between genome architecture and gene family evolution in ciliates. *mBio*, **10**(6): e02524–19.
- Yan Y, Rogers AJ, Gao F, Katz LA. 2017. Unusual features of non-dividing somatic macronuclei in the ciliate class Karyorelictea. *European Journal of Protistology*, **61**: 399–408.
- Yan Y, Xu Y, Al-Farraj SA, Al-Rasheid KAS, Song WB. 2016. Morphology and phylogeny of three trachelocercids (Protozoa, Ciliophora, Karyorelictea), with description of two new species and insight into the evolution of the family Trachelocercidae. *Zoological Journal of the Linnean Society*, **177**(2): 306–319.
- Yan Y, Xu Y, Yi ZZ, Warren A. 2013. Redescriptions of three trachelocercid ciliates (Protista, Ciliophora, Karyorelictea), with notes on their phylogeny based on small subunit rRNA gene sequences. *International Journal of Systematic and Evolutionary Microbiology*, **63**(9): 3506–3514.



## Supplementary Materials

**Supplementary Table S1** Sequence comparisons of SSU rDNA sequences determined by BioEdit v7.0.5.

SSU rDNA sequence	1	2	3	4	5	6	7	8	9
1. <i>Remanella rugosa</i>	-	96.5	96.2	97.2	96.1	100	87.2	94.2	98.1
2. <i>Remanella elongata</i> <b>sp. nov.</b>	53	-	95.7	95.8	95.7	96.5	86.9	95.4	96.3
3. <i>Remanella aposinica</i> <b>sp. nov.</b>	58	66	-	96.3	99.6	96.2	87.3	94.3	96.4
4. <i>Remanella unicorpusculata</i>	43	64	56	-	96.2	97.2	88.2	94.2	96.8
5. <i>Remanella sinica</i>	60	66	6	58	-	96.1	87.3	94.4	96.2
6. <i>Remanella</i> sp. JX015378	0	53	57	42	60	-	87.4	94.2	98.1
7. <i>Remanella</i> sp. JX015377	198	202	196	182	196	197	-	85.9	87.4
8. <i>Remanella caudata</i>	89	71	87	89	86	89	218	-	94.1
9. <i>Remanella granulosa</i>	29	56	54	49	58	29	192	90	-

Values below diagonal are numbers of unmatched sites, values above diagonal are sequence similarities in percentage (%).